Laser Doppler Velocimetry (LDV) Measurements

Instrumentation:

a. Laser, Probe and Processor

Off surface flow field measurements were acquired via Laser Doppler velocimetry (LDV) which is a non-intrusive flow field diagnostic technique. The laser used in this system is a Spectra Physics Stabilite 2017 Argon Ion Laser. It is used in conjunction with a two-component Dantec Dynamics Fiber Flow laser Doppler velocimetry system. The Doppler bursts were measured using a BSA F60 Flow processor and BSA Flow Software Version 4.10 followed by Version 6.5. The processor was operated in coincidence mode so that all samples collected could be used in determining the Reynolds stress correlations. The Fiber Flow system splits the laser beam into two different wavelengths, a blue beam with wavelength of 532 nm and a green beam with wavelength of 488 nm. After the beams are split, and one is shifted by a constant 40 MHz via a Bragg cell to unambiguously detect flow direction. The fiber optic LDV system was operated in 180-degree backscatter mode. Two different focal length lenses were used on the 2D 60 mm fiber optic probe head. A 600 mm focal length lens was used for all profiles taken on the center-span location. For many of the off-span profiles, a 400 mm focal length lens was utilized for its ability to yield higher data rates, subsequently speeding up the data collection process. A photograph of the LDV system in operation is shown in Figure 1 below.

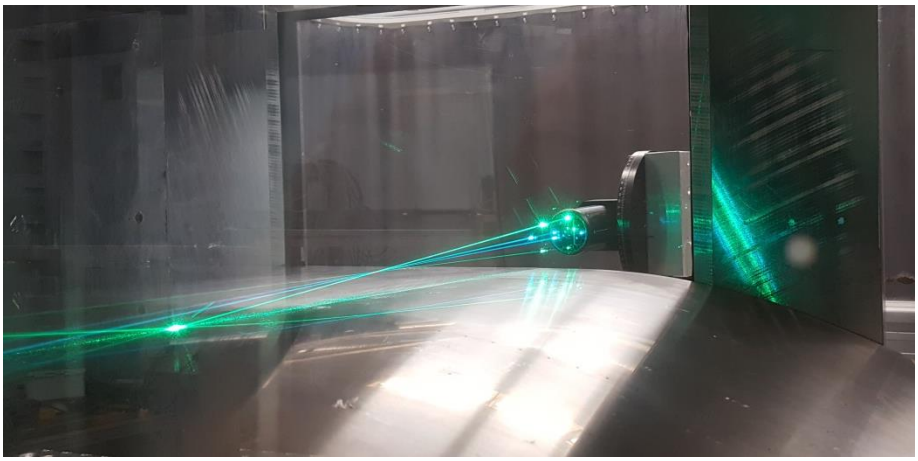

Figure 1 Photograph of the LDV system, utilizing the 400 mm lens, in operation taking a profile at the start of the ramp, X = 0.

b. Alignment Procedure:

In order to obtain near wall measurements, the LDV probe head was tilted by a small angle (angle, φ, in Figure 2) to align the bottom beam nearly parallel to the ramp surface. This corresponds to the alignment of the wall-normal component of velocity being tilted approximately 3°-7° to the normal direction, which was deemed negligible. The probe measurement volume has a wall-normal dimension of approximately 0.35 mm and 0.78 mm for the 400 mm and 600 mm focal length lenses respectively. This sets the effective spatial resolution of the mean and turbulent stress measurements. The utilized offset height of each first point should be approximately half of the probe wall-normal dimension (i.e. 0.35/2 = 0.18 mm and 0.78/2 = 0.39 mm), however, the data

sets were calculated using a prior value of 0.38/2 = 0.19 mm. This difference may easily be adjusted by the user by shifting the data, although this difference is likely within the uncertainty of the starting position which is estimated as dy = ±0.25 mm (the step value used in the alignment process).

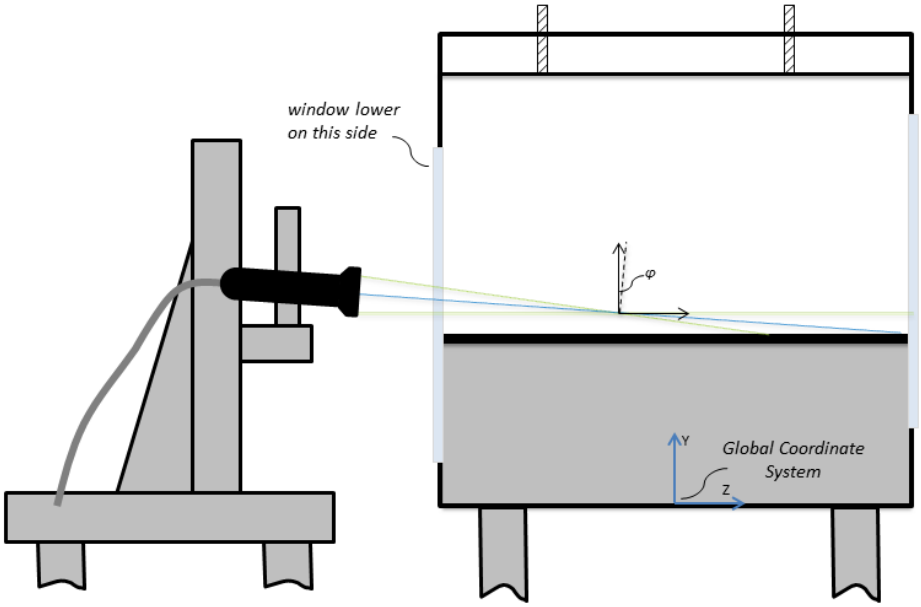

Figure 2 Schematic of LDV probe alignment relative to test section. Note, the image is oriented looking downstream.

c. Traverse and Controller:

A three-axis Aerotech traverse system was utilized in conjunction with a Unidex 11S controller. The controller uses the DM6006 Stepping Drive Module with 300SM / ES12271 stepper motors and a Parker Positioning systems linear sled. The system has a minimum of 200 steps/rev with 1 rev = 5 mm. This yields a resolution of 0.025 mm per step. Due to an inoperable axis of the controller, only two axes were able to be utilized at a time. Hence, for each wall-normal profile the z-axis of the traverse was positioned manually before the start of the run. It is estimated that the uncertainty for manual alignment is dz = ±2 mm however, since the flow is quasi two-dimensional, its sensitivity in this spanwise direction is very small.

The traverse was positioned on the lab floor with casters and then lifted via solid threaded feet such that its position was stationary during the entire measurement process. Due to vibration of the test section the actual location of the LDV probe volume varied relative to the model geometry, hence the uncertainty in the measurement location is larger than the traverse resolution.

Table 1 Uncertainty of traverse axes for controller aligned and manual alignment.

Axis	Controller Alignment Uncertainty (mm)	Manual Alignment Uncertainty (mm)
$\mathbf{X_{CI}, Y_{CI}, Z_{CI}}$	±0.025	±2

d. Seeding Particles:

The wind tunnel was seeded with Di-Ethyl-Hexyl-Sebacot (DEHS) particles of nominally 1-micron diameter using a TSI Six-Jet Atomizer 9306 high volume liquid droplet seeding generator. Typically, only three or four jets, of the six, were used at a time. Seeding particles were introduced locally wall-normal in the upstream internal inlet contraction. See the Experimental Facility document for more details on how the seeding particles were introduced into the flow.

Data Acquisition Procedures:

The data presented here were acquired over the period of approximately 17 months ranging from April 2018 to August 2019. For each test, the tunnel was warmed up and allowed to reach steady state before any LDV measurements were acquired. For each profile, the probe locations were preset in the BSA flow software and the data collection process was semi-automated. A typical profile took anywhere from 30 minutes to 3 hours to collect sufficient statistically converged data. The number of samples collected per probe location varied significantly due to a highly varying data rate throughout the flow measurement region. In many cases, multiple runs were acquired for a particular profile and the results were then ensemble averaged. Dantec BSA Flow Software versions 4.10 and 6.5 were used to acquire and process the raw signal. The data output for each probe location consisted of a separate text file containing the row#, arrival time [ms], transit time [ms], and the instantaneous streamwise u [m/s] and wall-normal, v [m/s] velocity components for each sample.

Processing of Data:

The individual text files for each probe location were loaded into and processed in MATLAB. The mean velocities were calculated as follows:

$$\bar{U} = \frac{\sum_{j=1}^{N} u_j}{N} \tag{1.1a}$$

$$\bar{V} = \frac{\sum_{j=1}^{N} v_j}{N} \tag{1.1b}$$

where u_j and v_j is the instantaneous velocity measurement of the data set and N is the number of samples. The variance is calculated as follows:

$$\overline{u'^2} = \frac{\sum_{j=1}^{N} |u_j - \bar{U}|^2}{N-1} \tag{1.1c}$$

$$\overline{v'^2} = \frac{\sum_{j=1}^{N} |v_j - \bar{V}|^2}{N-1} \tag{1.1d}$$

and the covariance as:

$$\overline{u'v'} = \frac{\sum_{j=1}^{N} (u_j - \bar{U})(v_j - \bar{V})}{N-1} \tag{1.1e}$$

Using these statistical quantities, the raw data was then filtered to remove any samples outside of three standard deviations from the mean, to minimize errors as suggested by DeGraaff and Eaton [1], and new statistical quantities were calculated to replace those acquired using the raw data. All these quantities are local ones calculated directly from the filtered time series data. In order to determine the coordinate locations and the statistical quantities in the global coordinate system, a

rotation must be applied to the local data. In the general sense, this is shown in Figure 3 where a coordinate system (x,y,z) is rotated to a reference frame (x_{ref},y_{ref},z_{ref}). The angle of the local coordinate system is α and the angle of the reference coordinate system is θ_{ref}. Together their difference gives the required rotation angle to rotate a vector in the (x,y,z) frame to one in the (x_{ref},y_{ref},z_{ref}) frame.

$$\theta = \theta_{ref} - \alpha \tag{1.2}$$

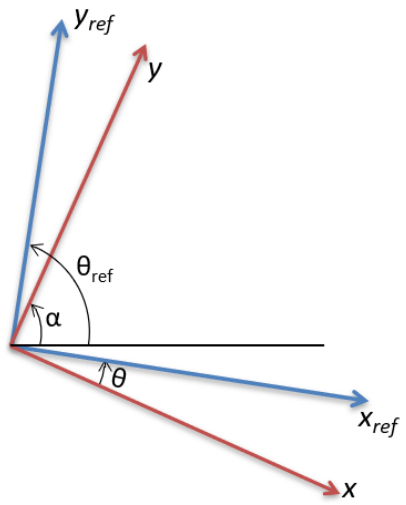

Figure 3 Local and reference coordinate system relations.

In this case, the reference coordinate system is the global one and $\theta_{ref} = \pi/2$. The angle of the local coordinate system, α, is calculated from the normal line of the ramp as follows:

$$\alpha(X) = \text{atan}\left(\frac{-1}{5a_4X^4+4a_3X^3+3a_2X^2}\right) \tag{1.3}$$

where the coefficients are given in terms of the ramp length, L = 0.9 m, the ramp height, H = 0.2 m and defined as:

$$a_2 = -10H/L^3, \quad a_3 = 15H/L^4, \quad a_4 = -6H/L^5 \tag{1.4}$$

Note that α is a function of X and for each rotation, the starting X-location of the profile, X_p, must be used to calculate α. Here the rotation consists of rotating the local quantities in the (x,y,z) coordinate system through the angle θ to the global coordinate system (X,Y,Z). First the local (x,y,z) coordinates were rotated to the global coordinate system using the a first order tensor rotation

$$X_G = R^T \cdot X_L + X_{offset} \tag{1.5}$$

where X_G is the coordinate vector in the global coordinates and X_L is the coordinate vector in the local coordinates and X_{offset} is the translation of the origin. Here X_G, X_L and X_{offset} are defined as

$$X_G = \begin{bmatrix} X \\ Y \\ Z \end{bmatrix} \quad and \quad X_L = \begin{bmatrix} x \\ y \\ z \end{bmatrix} \quad and \quad X_{offset} = \begin{bmatrix} X_p \\ f(X_p) \\ 0 \end{bmatrix} \tag{1.6}$$

and R is the rotation matrix defined as

$$R = \begin{bmatrix} \cos(\theta) & -\sin(\theta) & 0 \\ \sin(\theta) & \cos(\theta) & 0 \\ 0 & 0 & 1 \end{bmatrix} \tag{1.7}$$

The mean velocities were then calculated in the global coordinate system using a similar first order tensor rotation defined as follows:

$$U_G = R^T \cdot U_L \tag{1.8}$$

where U_G is the mean velocity vector in the global coordinates and U_L is the mean velocity vector in the local coordinates. Here U_G and U_L are defined as:

$$U_G = \begin{bmatrix} U_{global} \\ V_{global} \\ 0 \end{bmatrix} \quad and \quad U_L = \begin{bmatrix} U_{local} \\ V_{local} \\ 0 \end{bmatrix} \tag{1.9}$$

Finally, the stresses were calculated in the global coordinate system using a second order tensor rotation defined as

$$T_G = R^T \cdot T_L \cdot R \tag{1.10}$$

where T is the Reynolds stress tensor defined as follows:

$$T = \begin{bmatrix} \overline{u'^2} & \overline{u'v'} & 0 \\ \overline{u'v'} & \overline{v'^2} & 0 \\ 0 & 0 & 0 \end{bmatrix} \tag{1.11}$$

and the subscripts L and G refer to the local and global coordinate systems respectively.

Uncertainty Analysis:

The uncertainty analysis procedure followed the general guidelines laid out in the ASME PTC 19.1-2005 Test Uncertainty manual [2]. First the uncertainty of the statistical quantities in the local coordinate system will be presented followed by that of the global coordinate system.

Uncertainty Analysis – Local Values

a. Random Uncertainty

Random standard uncertainties were calculated based off the guidelines of Benedict and Gould [3] as they apply to data fitting any probability distribution and not just the normal distribution. The random standard uncertainties are related to the estimator variances as follows:

$$s_{\overline{U}} = \sqrt{\frac{\overline{u'^2}}{N}} \tag{2.1a}$$

$$s_{\overline{V}} = \sqrt{\frac{\overline{v'^2}}{N}} \tag{2.1b}$$

$$s_{\overline{u'^2}} = \sqrt{\frac{\overline{u'^4} - \overline{u'^2}}{N}} \tag{2.1.c}$$

$$s_{\overline{v'^2}} = \sqrt{\frac{\overline{v'^4} - \overline{v'^2}}{N}} \tag{2.1d}$$

$$s_{\overline{u'v'}} = \sqrt{\frac{\overline{u'^2v'^2} - \left(\overline{u'v'}\right)^2}{N}} \tag{2.1e}$$

This next part documents how the systematic uncertainties were accounted for.

b. Filtering Uncertainty

The first systematic uncertainty accounted for is that due to filtering the raw data as suggested by DeGraaff and Eaton [1]. A filtering uncertainty was based on the difference between the raw variables and the filtered ones. This uncertainty is nonsymmetric, so the procedure outlined in section 8-2 of the ASME PTC 19.1-2005 Test Uncertainty manual [2] was followed. The systematic standard uncertainty is written as:

$$b_{\overline{U}_f} = \frac{\overline{U}_{raw} - \overline{U}}{2} \tag{2.2a}$$

$$b_{\overline{V}_f} = \frac{\overline{V}_{raw} - \overline{V}}{2} \tag{2.2b}$$

$$b_{\overline{u'^2}_f} = \frac{\overline{u'^2}_{raw} - \overline{u'^2}}{2} \tag{2.2c}$$

$$b_{\overline{v'^2}_f} = \frac{\overline{v'^2}_{raw} - \overline{v'^2}}{2} \tag{2.2d}$$

$$b_{\overline{u'v'}_f} = \frac{\overline{u'v'}_{raw} - \overline{u'v'}}{2} \tag{2.2e}$$

where the coverage factor was taken as $k_f = \sqrt{3}$. The offset of each of the measurements is defined as follows:

$$q_{\overline{U}_f} = \frac{\overline{U}_{raw} - \overline{U}}{2} \tag{2.3a}$$

$$q_{\overline{V}_f} = \frac{\overline{V}_{raw} - \overline{V}}{2} \tag{2.3b}$$

$$q_{\overline{u'^2}_f} = \frac{\overline{u'^2}_{raw} - \overline{u'^2}}{2} \tag{2.3c}$$

$$q_{\overline{v'^2}_f} = \frac{\overline{v'^2}_{raw} - \overline{v'^2}}{2} \tag{2.3d}$$

$$q_{\overline{u'v'}_f} = \frac{\overline{u'v'}_{raw} - \overline{u'v'}}{2} \tag{2.3e}$$

c. Temperature Variation Uncertainty

The temperature varies throughout the duration of each run thereby changing the local speed of sound. Since the Mach number, *M* is held constant at 0.2 throughout the duration of the tests, the freestream velocity must change in proportion to the local changes in the speed of sound. This introduces uncertainty that may be accounted for by examining the relationship between freestream velocity, *U*, and temperature, *T*, via the definition of the Mach number, *M*, written as:

$$\overline{U} = M\sqrt{\gamma RT} \tag{2.4a}$$

The sensitivity of this term can be written as:

$$\frac{\partial \bar{U}}{\partial T} = \frac{M}{2}\sqrt{\frac{\gamma R}{T}} \tag{2.4b}$$

or equivalently,

$$b_{\overline{U_T}} = \frac{\partial U}{\partial T} b_T = \frac{M}{2}\sqrt{\frac{\gamma R}{T}} b_T \tag{2.4c}$$

where b_T is the uncertainty in temperature taken as half the estimated greatest change in temperature over the course of all the tests. Similarly, the wall-normal component of velocity, *V*, would be affected by the changing temperature. Here we estimate its uncertainty as follows:

$$b_{\overline{V_T}} = \frac{\bar{V}}{\bar{U}}\frac{\partial \bar{U}}{\partial T} b_T = \frac{\bar{V}}{\bar{U}}\frac{M}{2}\sqrt{\frac{\gamma R}{T}} b_T \tag{2.4d}$$

d. Calibration Uncertainty

The uncertainties listed so far are all dependent on the experiment, i.e. the number of samples, the type of post-process filtering, and the temperature variation during the test. Eliminating these, there is still a calibration uncertainty inherent with the LDV hardware and software, (i.e. how based on the inherent accuracy of the system). A typical method to calibrate LDV systems is to use a small wire on the edge of a rotating disk. The LDV probe volume is set coincident to the edge of the disk and a burst is detected each time the wire breaks the probe volume. By accurately knowing the diameters of the wire and disk and the rotation rate, the LDV system uncertainty can be estimated. Results from a NIST calibration on a similar Dantec Dynamics LDV system was used to estimate the calibration uncertainty. The uncertainty is taken from [6] and given as a function of velocity and is applied here to both LDV components as:

$$b_{\bar{U}_c}(\bar{U}) = \sqrt{(0.0032\bar{U})^2 + (0.0018)^2} \tag{2.5a}$$

$$b_{\bar{V}_c}(\bar{V}) = \sqrt{(0.0032\bar{V})^2 + (0.0018)^2} \tag{2.5b}$$

Again, this calibration uncertainty is only an estimate based on a similar calibration procedure.

e. Instrument Uncertainty

There is inherent uncertainty associated with the settings of the LDV flow processer, dubbed here as the instrument uncertainty. These settings include sensitivity, signal gain, signal to noise ratio, velocity span etc. With the most stringent settings, in theory, the instrument uncertainty should approach zero; however, frequently these settings had to be adjusted to off-ideal values as the data rate would otherwise fall to zero. There is no standard procedure for quantifying this uncertainty and our attempts would be speculative at best. Here we only acknowledge the existence of this uncertainty component but do not include it in the analysis.

f. Velocity Bias Uncertainty

Another source that introduces uncertainty into the measurement is that stemming from velocity bias. DeGraaff and Eaton [1] describe velocity bias as, “assuming the particles are uniformly distributed in the fluid, the likelihood of a particle passing through the measurement volume is proportional to the fluid velocity”. Weighting methods exist to compensate for this bias, but they are only viable in high data rate scenarios, which is not the case here. In low data rate scenarios there is no consensus on the best approach to quantify the velocity bias [4]. The Dantec

reference manual [5] states that if the samples are statistically independent then weighting methods are unnecessary as the standard weighting of 1/N is sufficient. Here we acknowledge the velocity bias uncertainty, which is likely to be quite small in this case, but do not attempt to account for it in this analysis.

g. Validation Bias Uncertainty

Also known as filter bias, validation bias is "the tendency of real systems to have a measurement efficiency that is dependent on the speed of the measured particle" [4]. There is no universal approach to handle validation bias as it is too system dependent. Again, this uncertainty is simply acknowledged but not accounted for here.

h. Systematic Standard Uncertainty

The systematic standard uncertainty is a combination of all the individual systematic uncertainties and coverage factors and is calculated as follows:

$$b_{\overline{U}} = \left[\left(\frac{1}{k_f} b_{\overline{U_f}}\right)^2 + \left(\frac{1}{k_c} b_{\overline{U_c}}\right)^2 + \left(\frac{1}{k_T} b_{\overline{U_T}}\right)^2\right]^{\frac{1}{2}} \tag{2.6a}$$

$$b_{\overline{V}} = \left[\left(\frac{1}{k_f} b_{\overline{V_f}}\right)^2 + \left(\frac{1}{k_c} b_{\overline{V_c}}\right)^2 + \left(\frac{1}{k_T} b_{\overline{V_T}}\right)^2\right]^{\frac{1}{2}} \tag{2.6b}$$

$$b_{\overline{u'^2}} = \left[\left(\frac{1}{k_f} b_{\overline{u'^2}_f}\right)^2\right]^{\frac{1}{2}} \tag{2.6c}$$

$$b_{\overline{v'^2}} = \left[\left(\frac{1}{k_f} b_{\overline{v'^2}_f}\right)^2\right]^{\frac{1}{2}} \tag{2.6d}$$

$$b_{\overline{u'v'}} = \left[\left(\frac{1}{k_f} b_{\overline{u'v'}_f}\right)^2\right]^{\frac{1}{2}} \tag{2.6e}$$

Unless otherwise specified, the distributions were not assumed to be known so the coverage factors were taken as $k = \sqrt{3}$.

i. Combined and Expanded Uncertainties

The combined standard uncertainty is a combination of the random uncertainty and the systematic standard uncertainty.

$$x_{\overline{U}} = \left[\, b_{\overline{U}}^2 + s_{\overline{U}}^2\right]^{\frac{1}{2}} \tag{2.7a}$$

$$x_{\overline{V}} = \left[\, b_{\overline{V}}^2 + s_{\overline{V}}^2\right]^{\frac{1}{2}} \tag{2.7b}$$

$$x_{\overline{u'^2}} = \left[\, b_{\overline{u'^2}}^2 + s_{\overline{u'^2}}^2\right]^{\frac{1}{2}} \tag{2.7c}$$

$$x_{\overline{v'^2}} = \left[\, b_{\overline{v'^2}}^2 + s_{\overline{v'^2}}^2\right]^{\frac{1}{2}} \tag{2.7d}$$

$$x_{\overline{u'v'}} = \left[b_{\overline{u'v'}}^2 + s_{\overline{u'v'}}^2 \right]^{\frac{1}{2}} \tag{2.7e}$$

The expanded uncertainty is the combined standard uncertainty multiplied by the Student's t-table value, $t_{v,p}$ where v is $N - 1$ and p is the selected confidence interval. At 20:1 odds or p = 95% confidence and assuming a large sample size, $t_{v,p}$ = 1.96. For all of the reported values, $t_{v,p}$ was calculated based off of the actual number of samples in the data set and hence in some cases was larger than 1.96. Using this analysis, the 95% confidence intervals are:

$$\overline{U}_{95} = \pm t_{v,p} x_{\overline{U}} \tag{2.8a}$$

$$\overline{V}_{95} = \pm t_{v,p} x_{\overline{V}} \tag{2.8b}$$

$$\overline{u'^2}_{95} = \pm t_{v,p} x_{\overline{u'^2}} \tag{2.8c}$$

$$\overline{v'^2}_{95} = \pm t_{v,p} x_{\overline{v'^2}} \tag{2.8d}$$

$$\overline{u'v'}_{95} = \pm t_{v,p} x_{\overline{u'v'}} \tag{2.8e}$$

where $t_{v,p}$ x_i is the expanded uncertainty. The final asymmetric 95% confidence intervals can then be written as:

$$\overline{U}_{lower\ limit} = \overline{U} + q_{\overline{U}_f} - \overline{U}_{95} \tag{2.9a}$$

$$\overline{U}_{upper\ limit} = \overline{U} + q_{\overline{U}_f} + \overline{U}_{95} \tag{2.9b}$$

$$\overline{V}_{lower\ limit} = \overline{V} + q_{\overline{V}_f} - \overline{V}_{95} \tag{2.9c}$$

$$\overline{V}_{upper\ limit} = \overline{V} + q_{\overline{V}_f} + \overline{V}_{95} \tag{2.9d}$$

$$\overline{u'^2}_{lower\ limit} = \overline{u'^2} + q_{\overline{u'^2}_f} - \overline{u'^2}_{95} \tag{2.9e}$$

$$\overline{u'^2}_{upper\ limit} = \overline{u'^2} + q_{\overline{u'^2}_f} + \overline{u'^2}_{95} \tag{2.9f}$$

$$\overline{v'^2}_{lower\ limit} = \overline{v'^2} + q_{\overline{v'^2}_f} - \overline{v'^2}_{95} \tag{2.9g}$$

$$\overline{v'^2}_{upper\ limit} = \overline{v'^2} + q_{\overline{v'^2}_f} + \overline{v'^2}_{95} \tag{2.9h}$$

$$\overline{u'v'}_{lower\ limit} = \overline{u'v'} + q_{u'v'_f} - \overline{u'v'}_{95} \tag{2.9i}$$

$$\overline{u'v'}_{upper\ limit} = \overline{u'v'} + q_{\overline{u'v'}_f} + \overline{u'v'}_{95} \tag{2.9j}$$

where the q_i's are the offset given by equations (2.3a-e).

Uncertainty Analysis – Global Values:

For the global coordinate system, Section 7 of the ASME PTC 19.1-2005 Test Uncertainty manual [2] was followed to propagate the uncertainties calculated for the local coordinate system into the global coordinate system. The functional dependence of the mean and turbulence quantities in the global coordinate system on those acquired in the local coordinate system is as follows:

$$\overline{U_G} = f(\overline{U_L}, \overline{V_L}) \tag{3.1a}$$

$$\overline{V_G} = f(\overline{U_L}, \overline{V_L}) \tag{3.1b}$$

$$\overline{u_G'^2} = f(\overline{u_L'^2}, \overline{v_L'^2}, \overline{u'v_L'}) \tag{3.1c}$$

$$\overline{v_G'^2} = f(\overline{u_L'^2}, \overline{v_L'^2}, \overline{u'v_L'}) \tag{3.1d}$$

$$\overline{u'v_G'} = f(\overline{u_L'^2}, \overline{v_L'^2}, \overline{u'v_L'}) \tag{3.1e}$$

The sensitivities of each global value with respect to its dependent local values may be obtained by partial differentiation. For example, the sensitivities of Eq. (3.1a) are

$$\frac{\partial \overline{U_G}}{\partial \overline{U_L}} = \frac{\partial}{\partial U_L}(R^T \cdot U_L) = R_{11}^T \tag{3.2a}$$

$$\frac{\partial \overline{U_G}}{\partial \overline{V_L}} = \frac{\partial}{\partial V_L}(R^T \cdot U_L) = R_{12}^T \tag{3.2b}$$

where Eq. (1.8) is used. Similar results are obtained for Eqs. (3.1b)- (3.1e).

Using the sensitivities, the random uncertainties are:

$$S_{\overline{U_G}} = \left[(R_{11}^T S_{\overline{U_L}})^2 + (R_{12}^T S_{\overline{V_L}})^2\right]^{\frac{1}{2}} \tag{3.3a}$$

$$S_{\overline{V_G}} = \left[(R_{21}^T S_{\overline{U_L}})^2 + (R_{22}^T S_{\overline{V_L}})^2\right]^{\frac{1}{2}} \tag{3.3b}$$

$$S_{\overline{u_G'^2}} = \left[(R_{11}R_{11}S_{\overline{u_L'^2}})^2 + (R_{21}R_{21}S_{\overline{v_L'^2}})^2 + (R_{11}R_{21}S_{\overline{u'v_L'}})^2\right]^{\frac{1}{2}} \tag{3.3c}$$

$$S_{\overline{v_G'^2}} = \left[(R_{12}R_{12}S_{\overline{u_L'^2}})^2 + (R_{22}R_{22}S_{\overline{v_L'^2}})^2 + (R_{12}R_{22}S_{\overline{u'v_L'}})^2\right]^{\frac{1}{2}} \tag{3.3d}$$

$$S_{\overline{u'v_G'}} = \left[(R_{11}R_{12}S_{\overline{u_L'^2}})^2 + (R_{21}R_{22}S_{\overline{v_L'^2}})^2 + (R_{11}R_{22}S_{\overline{u'v_L'}})^2\right]^{\frac{1}{2}} \tag{3.3e}$$

where the subscripts ‘L’ and ‘G’ refer to the local and global coordinate value respectively and are added purely for clarity. Note that the local random uncertainties of equations (2.1a-e) did not have ‘L’ subscripts even though they do here.

The systematic standard uncertainties have the same form as the random uncertainties and are given as:

$$b_{\overline{U_G}} = \left[(R_{11}^T b_{\overline{U_L}})^2 + (R_{12}^T b_{\overline{V_L}})^2\right]^{\frac{1}{2}} \tag{3.4a}$$

$$b_{\overline{V_G}} = \left[(R_{21}^T b_{\overline{U_L}})^2 + (R_{22}^T b_{\overline{V_L}})^2\right]^{\frac{1}{2}} \tag{3.4b}$$

$$b_{\overline{u_G'^2}} = \left[(R_{11}R_{11}b_{\overline{u_L'^2}})^2 + (R_{21}R_{21}b_{\overline{v_L'^2}})^2 + (R_{11}R_{21}b_{\overline{u'v_L'}})^2\right]^{\frac{1}{2}} \tag{3.4c}$$

$$b_{\overline{v_G'^2}} = \left[(R_{12}R_{12}b_{\overline{u_L'^2}})^2 + (R_{22}R_{22}b_{\overline{v_L'^2}})^2 + (R_{12}R_{22}b_{\overline{u'v_L'}})^2\right]^{\frac{1}{2}} \tag{3.4d}$$

$$b_{\overline{u'v'_G}} = \left[(R_{11}R_{12}b_{\overline{u'^2_L}})^2 + (R_{21}R_{22}b_{\overline{v'^2_L}})^2 + (R_{11}R_{22}b_{\overline{u'v'_L}})^2\right]^{\frac{1}{2}} \quad (3.4e)$$

Note again that the subscripts 'L' and 'G' refer to the local and global coordinate values respectively and are added purely for clarity.

Combined and Expanded Uncertainties

The combined and expanded uncertainties take on the same form as for the local values with the new global random and systematic standard uncertainty values replacing the local ones. The only change that occurs is that the offset quantities of each of the measurements are changed from their respective local values to the following global ones:

$$q_{G_{\bar{U}}} = f\left(\overline{U_L} + q_{\bar{U}_f}, \overline{V_L} + q_{\bar{V}_f}\right) - f(\overline{U_L}, \overline{V_L}) \quad (3.5a)$$

$$q_{G_{\bar{V}}} = f\left(\overline{U_L} + q_{\bar{U}_f}, \overline{V_L} + q_{\bar{V}_f}\right) - f(\overline{U_L}, \overline{V_L}) \quad (3.5b)$$

$$q_{G_{\overline{u'^2}}} = f\left(\overline{u'^2_L} + q_{\overline{u'^2}_f}, \overline{v'^2_L} + q_{\bar{v}_f}, \overline{u'v'_L} + q_{\overline{u'v'}_f}\right) - f(\overline{u'^2_L}, \overline{v'^2_L}, \overline{u'v'_L}) \quad (3.5c)$$

$$q_{G_{\overline{v'^2}}} = f\left(\overline{u'^2_L} + q_{\overline{u'^2}_f}, \overline{v'^2_L} + q_{\bar{v}_f}, \overline{u'v'_L} + q_{\overline{u'v'}_f}\right) - f(\overline{u'^2_L}, \overline{v'^2_L}, \overline{u'v'_L}) \quad (3.5d)$$

$$q_{G_{\overline{\overline{u'v'}}}} = f\left(\overline{u'^2_L} + q_{\overline{u'^2}_f}, \overline{v'^2_L} + q_{\bar{v}_f}, \overline{u'v'_L} + q_{\overline{u'v'}_f}\right) - f(\overline{u'^2_L}, \overline{v'^2_L}, \overline{u'v'_L}) \quad (3.5e)$$

where the functions *f* are from equations (3.1a-e).

References:

[1] DeGraaff, D. B., and Eaton, J. K. "A High-Resolution Laser Doppler Anemometer: Design, Qualification, and Uncertainty." *Experiments in Fluids*, Vol. 30, No. 5, 2001, pp. 522–530. doi:10.1007/s003480000231.

[2] *ASME PTC 19.1 - 2005 Test Uncertainty*. ASME, 2005.

[3] Benedict, L. H., and Gould, R. D. "Towards Better Uncertainty Estimates for Turbulence Statistics." *Experiments in Fluids*, Vol. 22, No. 2, 1996, pp. 129–136. doi:10.1007/s003480050030.

[4] Edwards, R. V. "Report of the Special Panel on Statistical Particle Bias Problems in Laser Anemometry." *Journal of Fluids Engineering*, Vol. 109, No. 2, 1987, pp. 89–93. doi:10.1115/1.3242646.

[5] LDA and PDA Reference Manual.

[6] Yeh, T. T., and Hall, J. M. "NIST Special Publication 250-79 Airspeed Calibration Service." *Special Publication (NIST SP) - 250-79*, 2007. doi:http://dx.doi.org/10.1002/https://dx.doi.org/10.6028/NIST.SP.250-79.